processes

MDPI

Article

Preparation and Characterization of Cinnamomum Essential Oil–Chitosan Nanocomposites: Physical, Structural, and Antioxidant Activities

Hongxia Su, Chongxing Huang *, Ying Liu, Song Kong, Jian Wang, Haohe Huang and Bobo Zhang

School of Light Industry & Food Engineering, Guangxi University, Nanning 530004, China; suhongxia@st.gxu.edu.cn (H.S.); sunflowersgxu@hotmail.com (Y.L.); stephen_K615@hotmail.com (S.K.); wjpgydyd@st.gxu.edu.cn (J.W.); huanghaohe@st.gxu.edu.cn (H.H.); zbobo05@163.com (B.Z.)

* Correspondence: huangcx@gxu.edu.cn; Tel.: +86-138-7818-7372

Received: 29 May 2020; Accepted: 9 July 2020; Published: 13 July 2020

Abstract: In this study, different amounts of cinnamomum essential oil (CEO) were encapsulated in chitosan nanoparticles (NPs) (CS-NPs) through oil-in-water emulsification and ionic gelation. An ultraviolet-visible spectrophotometer, Fourier-transform infrared spectroscopy, synchronous thermal analysis, and X-ray diffraction were employed to analyze the CEO encapsulation. As observed by field-emission scanning electron microscopy, NP size analysis and zeta potential, the prepared CS-NPs, containing CEO (CS-CEO), were spherical with uniformly distributed sizes (diameters: 190–340 nm). The ranges of encapsulation efficiency (EE) and loading capacity (LC) were 4.6–32.9% and 0.9–10.4%, with variations in the starting weight ratio of CEO to CS from 0.11 to 0.53 (*w*/*w*). It was also found that the antioxidant activity of the CS-NPs loaded with CEO increased as the EE increased. The active ingredients of the CEO were prevented from being volatilized, significantly improving the chemical stability. The antioxidant activity of CS-CEO was higher than that of the free CEO. These results indicate the promising potential of CS-CEO as an antioxidant for food processing, and packaging applications.

Keywords: cinnamomum essential oil; chitosan; encapsulation; antioxidant activity

1. Introduction

Owing to the potential hazards of artificial food additives to human health, natural, functional, and bioactive ingredients have drawn considerable attention because of their proven health benefits [1]. Essential oils (EOs) obtained from medicinal and herbal plants are recognized for their antioxidant properties. EOs from different herbs have been utilized as food flavors and medicines, and in the preparation of fragrances, which are volatile and fat-soluble [2–9]. The compositions of plant EOs are complex and contain high amounts of phenols, acetones, terpenes, alcohols, and aldehydes, which exhibit good antibacterial, antioxidant, and insecticidal properties. Although the pharmacological effects of EOs have long been known, their application in the food industry is still limited [10,11]. Cinnamomum EO (CEO), known for its strong inhibitory, microbicidal, and antioxidant properties, as well as other beneficial properties [12], is extracted from tree species that are widely distributed in the tropics and southern subtropical regions. Such properties are mainly due to the presence of cinnamaldehyde, eugenol (the main ingredient of CEO), and monoterpene hydrocarbons at low concentrations [13,14]. CEO has been proven to be a good antibacterial and antioxidant agent because of its volatility and ease of degradation under environmental or processing conditions (e.g., high temperature, low pressure, and presence of air and light), but its utilization in the maintenance of

food quality and reduction of food oxidation is limited [15]. Encapsulation is an effective strategy to improve the sensitivity to degradation and promote the stability of the biologically active compounds in CEO during the processing and storage stages [16].

Nanoencapsulation is an emerging technology among the various techniques employed for encapsulation; it is widely employed in the food and nutrition industries. The nanoencapsulation of biologically active compounds has been demonstrated as a reliable and effective approach toward increasing the physical and chemical stabilities of active substances, thereby protecting them from volatilization and harmful environmental conditions, and extending the shelf life of food [17]. Additionally, it can improve water solubility, control delivery, facilitate absorption, and reduce toxicity and cost [18]. Chitosan (CS) is a natural cationic polysaccharide with good biocompatibility, low toxicity, and excellent biodegradability, and is considered an ideal option for food packaging [19–22]. It has been reported that CS, as a nanoparticle (NP) carrier, can encapsulate EOs and improve their stability. Mustafa employed spray-drying technology to encapsulate oregano EO in CS-NPs [23]. The obtained particles exhibited good thermal stability and antifungal activity, and could be utilized as alternatives to synthetic preservatives in the agricultural sector. Khalili prepared NPs through the self-assembly of CS and sodium benzoate and encapsulated thyme EO in NPs [24]. It was found that fungus growth was completely inhibited at a pure EO concentration of 400 mg/L under sealed conditions. The same effect was achieved when the NPs were concentrated at 300 mg/L. It was found that NPs could significantly improve the stability and antifungal activity of thyme EO. Ali Mohammadi embedded eucalyptus EO in CS-NPs, which were applied on the surface of cucumber to significantly improve its physicochemical quality and prolong its shelf life [25]. Moreover, oxidation, as one of the important reactions that result in the corruption of food during processing and storage [26], shortens the shelf life of products by causing changes in flavor, texture, and color. Oxidation is not conducive to human health, and many reactive oxygen intermediates can induce a variety of diseases.

However, most of the aforementioned studies focused on the antibacterial properties of NPs and their food preservation applications. Research on the structure, physical properties, and oxidation resistance of NPs is still rare. Finally, to the best of our knowledge, the literature on the antioxidant activities of CEO encapsulated in CS nanoparticles is especially sparse.

This study aimed to prepare and characterize water-soluble CS-tripolyphosphate (TPP) NPs containing different amounts of CEO through oil-in-water emulsification and ion gelation techniques, which are nontoxic, convenient, and controllable [27]. The characteristics of the microcapsules were tested through encapsulation efficiency (EE), loading capacity (LC), particle size, zeta potential, scanning electron microscopy (SEM), Fourier-transform infrared (FT-IR) spectroscopy, and X-ray diffraction (XRD). Furthermore, the oxidation resistance of the CS-CEO was evaluated. This study aims to provide considerable advances in the fields of food and agriculture.

2. Materials and Methods

2.1. Materials

CS (deacetylation degree of 80–95%, viscosity of 50–800 mPa's) was purchased from Sinopharm Group Chemical Reagent Co., Ltd. (Beijing, China). CEO (purity of 90%) was purchased from Zhuhai Weijia Food Additive Co., Ltd. (Zhuhai, China). TPP and sodium hydroxide (analytical reagent grade) were purchased from Aladdin Industrial Co., Ltd. (Shanghai, China). Tween 80 (chemical grade) was purchased from Chengdu Kelong Chemical Reagent Co., Ltd. (Chengdu, China). Glacial acetic acid (chemical grade) and ethanol (purity of 90%) were purchased from Tianjin Zhiyuan Chemical Reagent Co., Ltd. (Tianjin, China).

2.2. Sample Preparation

2.2.1. CS-CEO

CS-CEO were prepared using the following steps. CS (0.28 mg) was added to an aqueous acetic acid solution (1% *v*/*v*, 40 mL) and stirred at 60 °C for 1 h, after which it was filtered through a 1 μm pore-sized filter. The pH of the preprepared CS solution was adjusted to 4.0–4.8 by 1 mol L^{-1} of sodium hydroxide. Then, Tween 80 (SN 45–55; 0.75% *w*/*v*) was added to the solution (40 mL) and stirred at 50 °C for 30 min to obtain a homogeneous mixture. Different amounts of CEO (0.03, 0.07, 0.11, and 0.15 g) were added to the homogeneous mixture and cooled to 25 °C [28–30].

TPP was dissolved in distilled water (0.15% *w*/*v*, 20 mL) [31], added dropwise to the fine, homogeneous emulsion (40 mL), and stirred for 30 min to form opalescent suspensions. NPs were collected by centrifugation at 10,000 rpm for 15 min at 25 °C and subsequently washed three times with water before being suspended via vortex mixing (15 s, vortex mixer XW-80A, The Haimen Lindberg Instrument Manufacturing Co., Ltd., Haimen, China). The obtained suspensions were immediately lyophilized at −58 °C for 48 h (vacuum freeze dryer, DGJ-10, Shanghai Bridge Feng Industrial Co., Ltd., Shanghai, China). Both the lyophilized CS-NPs and the suspensions were stored at 4 °C. Figure 1 illustrates the preparation of CS-CEO.

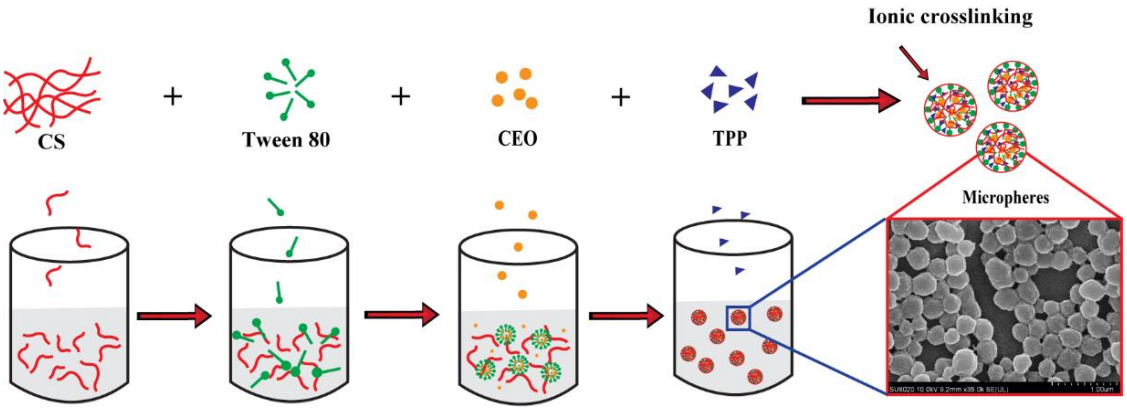

Figure 1. Process of preparing CS-CEO.

2.2.2. CS-NPs

The preparation of CS-NPs followed the same steps for preparing CS-CEO, without adding CEO.

2.3. Analytical Methods

2.3.1. EE and LC

The oil content of CS-CEO was tested using an ultraviolet-visible (UV-vis) spectrophotometer (SPECORD plus 50, Analytik Jena AG, Jena, Germany). The CEO standard was prepared in 95% absolute ethanol at a concentration range of 1–9 μg/mL. At a wavelength of 275 nm, the absorbance was measured using SPECORD plus 50, and a standard curve was drawn. An aliquot (3 mL) of the prepared suspension was added to an aqueous hydrochloric acid solution, uniformly mixed (2 mol L^{-1}, 30 mL), and heated in a water bath at 50 °C for 30 min. After cooling, it was transferred to a 50 mL volumetric flask containing 95% ethanol solution. The mixture was centrifuged at 10,000 rpm for 10 min at 25 °C, and the supernatant was collected. In sequence, the CEO content was measured, employing a UV-vis spectrophotometer at a wavelength of 275 nm. A blank CS-NP (without CEO) was also prepared. The CEO content was calculated using an appropriate standard curve of free CEO in a solvent of hydrochloric acid and ethanol, 2:1 *v*/*v* (R^2 = 0.999). The values for three samples were determined

for each experimental preparation, and the mean values were reported. EE and LC of CEO were calculated, employing Equations (1) and (2) [25].

$$\text{EE\%} = \frac{\text{Weight of loaded CEO}}{\text{Initial weight of CEO}} \times 100\% \quad (1)$$

$$\text{LC\%} = \frac{\text{Weight of loaded CEO}}{\text{Weight of sample}} \times 100\% \quad (2)$$

2.3.2. SEM

The morphology of the lyophilized NPs was analyzed by field-emission SEM (FE-SEM, SU-8020, Hitachi High-Technologies Co., Tokyo, Japan). The sample was plated with a thin layer of gold under high-vacuum conditions, and representative FE SEM images were obtained at different magnifications.

2.3.3. Particle Size

The particle sizes of both CS-NPs and CS-CEO were measured with an NP size analyzer (Nano ZSP, Malvern Instruments Co., Worcestershire, UK). The lyophilized NPs were suspended in distilled water and stirred in a water bath at 60 °C for 30 min. Following incubation, the suspension was filtered through 1 μm pore-sized filters, and the particle sizes were determined.

2.3.4. Zeta Potential Analysis

Solutions (water) containing 1 mg/mL of CS-NPs and CS-CEO were prepared, and the zeta potential was tested using an NP size analyzer (Nano ZSP, Malvern Instruments, Worcestershire, UK).

2.3.5. FT–IR

The structures of CS, pure CEO, CS-NPs, and CS-CEO were investigated by FT-IR, in the range of 400–4000 cm^{-1} (VERTEX 70 FT–IR, Bruker Corporation, Mannheim, Germany). The dried NPs were mixed with potassium bromide and pressed into discs to prepare a transparent sample.

2.3.6. Thermogravimetric Analysis (TGA)

Thermal analyses (TA) of the samples were conducted using a synchronous thermal analyzer (NETZSCH STA 449 F5, NETZSCH, Selb, Germany). Each of the prepared samples (7–10 mg) was placed in a standard aluminum crucible and heated at a stable rate of 10 °C min^{-1}. The temperature was raised from 25 to 600 °C with nitrogen as the shielding gas.

2.3.7. XRD

XRD patterns were obtained using an X-ray diffractometer (Smartlab 3 KW, Rigaku Corporation, Tokyo, Japan). The angle was varied over a 2θ range of 5–50° at a constant rate of 6° min^{-1}. The voltage and current were set to 40 kV and 40 mA.

2.3.8. Antioxidant Activity (AOA)

The antioxidant activities (AOAs) of the different amounts of CS-CEO were determined according to the following methods:

2,2-diphenyl-1-picrylhydrazyl (DPPH) free radical scavenging assay and
Hydroxyl free radical scavenging assay.

The DPPH free radical scavenging assay was performed as described previously (with some modifications) [32]. Samples (10 mg each) of CS-CEO (0.11:1, 0.25:1, 0.39:1, or 0.53:1 *w*/*w*) and CEO were suspended in ethanol (99%, 20 mL) to obtain a final concentration of 500 μg mL^{-1}. In sequence, they were vigorously stirred for 2 h to release the CEO. The mixture was then centrifuged at 25 °C for

10 min to obtain the supernatant for analysis. An aliquot of each supernatant (1 mL) of the mixture was mixed with the DPPH ethanol solution (0.0001 mol L^{-1}, 1 mL). After shaking, the mixture was left to react in a dark at room temperature for 2 h. The absorbance was measured at 517 nm by UV-vis spectroscopy. The CS-NPs of unloaded CEO were used as the control. The percentage of AOA was evaluated using Equation (3).

$$\mathrm{DDPH}_{\text{scavenging activity}}(\%) = \frac{\mathrm{A}_{\text{control}} - \mathrm{A}_{\text{sample}}}{\mathrm{A}_{\text{control}}} \times 100\%, \quad (3)$$

where $A_{control}$ and A_{sample} are the absorbances of the control and CEO-NP samples, respectively.

The hydroxyl radical scavenging activity was determined by the Fenton reaction, which tests the ability of mixtures to hydroxylate salicylates in the presence of NPs [33,34]. The test mixtures consisted of 1.0 mL of a CS-NP solution (loaded or unloaded with CEO) and CEO, 1.0 mL of $FeSO_4$ (6 mmol L^{-1}), 1.0 mL of H_2O_2 (6 mmol L^{-1}), and 1.0 mL of sodium salicylate (6 mmol L^{-1}). After incubation at 37 °C for 30 min, the absorbance of the mixture was measured at 510 nm. The hydroxyl radical scavenging activity was calculated, employing an equation which was similar to that of the DPPH assay (Equation (3)).

2.3.9. Statistical Analysis

The data were analyzed using analysis of variance (ANOVA) with the SPSS 23.0 program (SPSS Inc., Chicago, IL, USA). The statistical correlations were evaluated by Pearson's correlation coefficients, and a p-value < 0.05 was considered statistically significant. The figures were drawn using the Origin 8 program (OriginLab Co., Northampton, MA, USA).

3. Results and Discussion

3.1. EE and LC

The standard curve is shown in Figure 2 (y = 0.1212x + 0.2423 (R^2 = 0.9977)). From the UV-vis spectroscopy results, the EE and LC of CS-CEO, loaded at different initial weight ratios of CEO to CS (*w*/*w*), were calculated according to Equations (1) and (2). As observed in Table 1, the EE of CS-NPs ranged from 4.6% to 32.9%. With the initial increase in the CEO content, the EE also increased gradually, and the maximum value was obtained at a CEO to CS weight ratio of 0.39:1. However, when the amount of CEO increased further, the appearance of the mixture changed from milky white to light yellow, and the EE decreased. The decrease in EE due to the utilization of the highest tested initial weight ratio of CEO to CS might be interpreted as being a result of the concentrations of CS and TPP being constant and the formation of NPs being limited. The encapsulation of CEO reached saturation, and the excess CEO was free or adsorbed only on the surface of NPs. These findings are consistent with those of previous reports [35]. The LC of the CEO embedded in CS-NPs was in the range of 0.9–10.4% (Table 1). The data shown in Table 1 indicate an initial increase in LC with the increase of CEO content. However, in the third case, with the addition of CEO (0.15 g), the LC slightly decreased, i.e., from 10.4% to 10.3%. This result is consistent with those of previous studies on the encapsulation of carvacrol and eugenol in CS-TPP NPs [36–39].

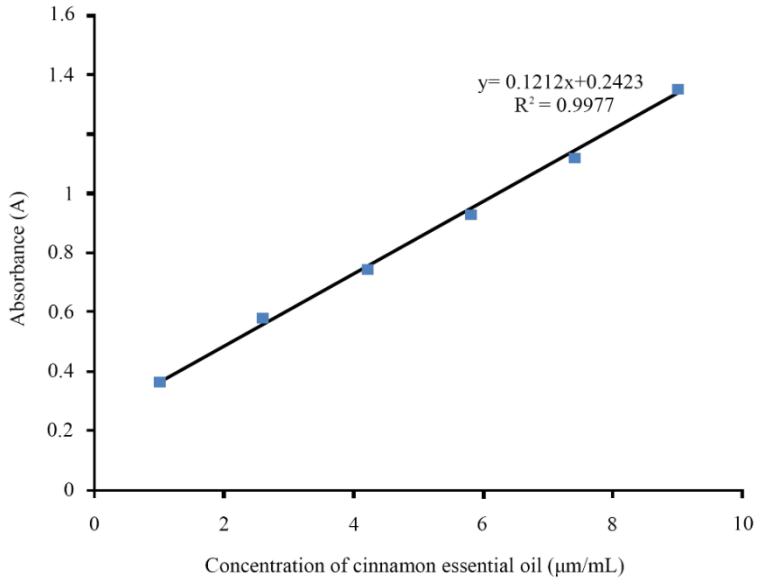

Figure 2. Standard CEO curves.

Table 1. EE and LC of CEO containing CS-NPs by UV–vis spectrophotometry.

NO	CEO: CS (*w*/*w*)	EE (%)	LC (%)
NP0	0:1	0	0
NP-A	0.11:1	4.6 ± 0.5	0.9 ± 0.3
NP-B	0.25:1	22.5 ± 1.5	7.8 ± 0.7
NP-C	0.39:1	32.9 ± 2.3	10.4 ± 0.7
NP-D	0.53:1	24.6 ± 0.5	10.3 ± 1.5

Results are reported as the mean ± SD, $n = 3$.

3.2. Characterization of CS-NPs by SEM, Particle Size Analyzer, Zeta Potentials, FT-IR, TGA, and XRD

The FE-SEM images effectively captured accurate information about the particle structure and morphology of the NP samples. Figure 3a,b show the FE-SEM images of CS-NPs, loaded and unloaded with CEO, respectively, at a CEO to a CS weight ratio of 0.39:1. As shown in Figure 3b, CS-NPs loaded with CEO were uniformly distributed in size, with a spherical shape, and the surface was smooth (without cracks), indicating that the CEO was well encapsulated in NPs.

The particle size distribution was also determined using a particle size analyzer (PSA), as shown in Figure 3c,d. The figures show that the average diameter of the CS-NPs is 100–140 nm. The CS-CEO exhibited an average diameter in the range of 190–340 nm. The particle size values, determined from the PSA images, were slightly higher than those measured by FE-SEM. This may be caused by the swelling of the CS layer or the aggregation of the NPs while they were dispersed in water [24]. With the addition of CEO, the particle size of the CS-NPs gradually became larger and the distribution became wider. This may be due to the embedding of CEO. Kavaz et al. obtained similar results in CS and Cyperus articulatus rhizome EOs [35].

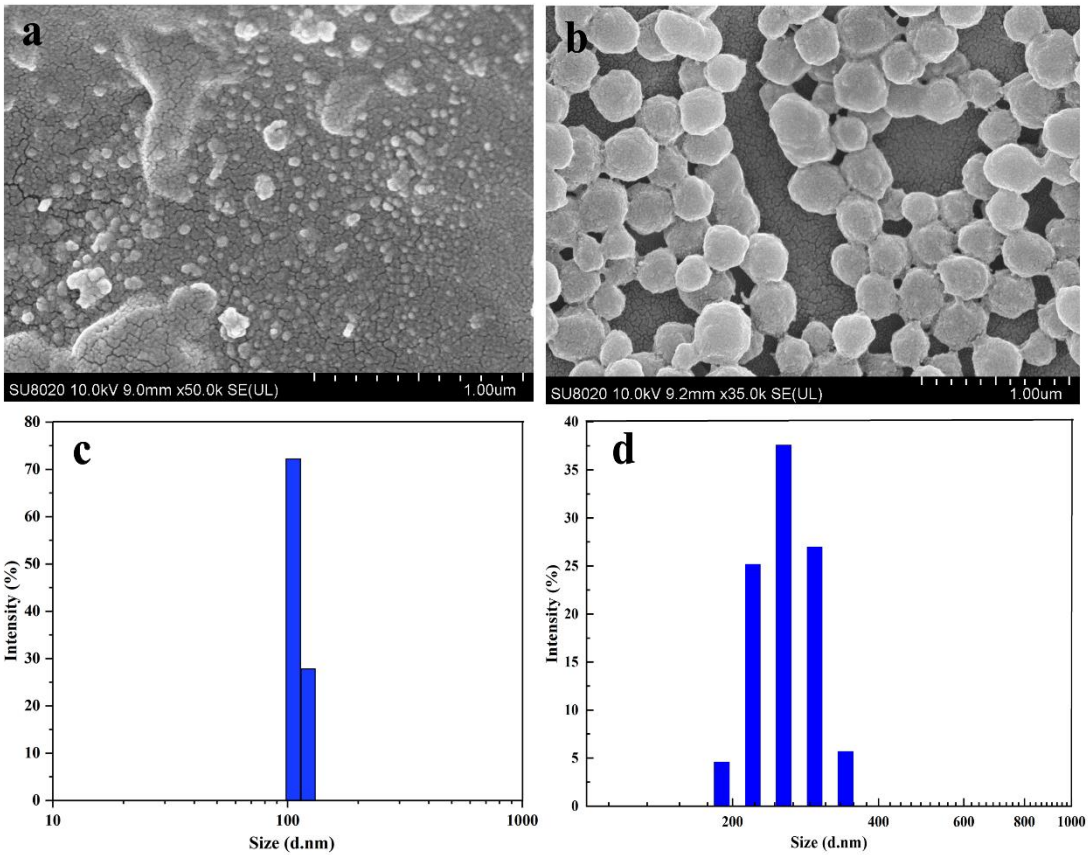

Figure 3. FE-SEM images of (**a**) CS-NP and (**b**) CS-CEO, at a CEO to CS weight ratio of 0.39:1 and magnification of 1.0×10^6. Particle size distribution of (**c**) CS-NPs and (**d**) CS-CEO loaded at a CEO to CS weight ratio of 0.39:1.

The potentials of the CS-NP and CS-CEO solutions, shown in Table 2, were 23.47 and 17.33 mV, respectively. With the embedding of the CEO, the potential of the CS-NP solution decreased due to the charge generated by the NPs containing EOs shielding the amino groups of CS. Similar results were obtained by Luque-Alcaraz et al. in CS and pepper tree Eos [40].

Table 2. Zeta potential of CS-NP and CS-CEO solutions.

Sample	Zeta Potential (mV)
CS-NP	23.47 ± 1.06
CS-CEO	17.33 ± 1.16

Figure 4 illustrates the FT-IR spectra of CS, CS-NPs, pure CEO, and CS-CEO. CS exhibited characteristic peaks at 3481 (–OH and $–NH_2$ stretching), 1642 (amide I band), 1553 (amide II, N-H bending), 1060 (C–O–C stretching), and 594 cm^{-1} (pyranoside ring stretching vibration). In the case of CS-NPs, the peak of amide II ($–NH_2$ bending) shifted from 1553 to 1536 cm^{-1}, and a new peak appeared at 1243 cm^{-1} (P = O); this indicates the formation of an ionic complex via the electrostatic interactions between the NH_3^+ groups of CS and the phosphate groups of TPP within CS-NPs [28]. The pure CEO spectra exhibited characteristic peaks at 2923 (C-H stretching), 1449 (CH_2 bending), 1119 (C–O–C stretching), and 891 cm^{-1} (C–H bending of the aromatic ring). All of the above characteristic peaks appeared in the spectra of CN-CEO NPs at similar wavenumbers, indicating that there was no measurable interaction between CEO and CS-NP. Moreover, compared to the FT–IR spectra of CS-NPs, the addition of CEO resulted in the appearance of a strong C-H bending mode absorption band of the aromatic ring at 891–792 cm^{-1}, verifying the presence of CEO within the CS-NPs.

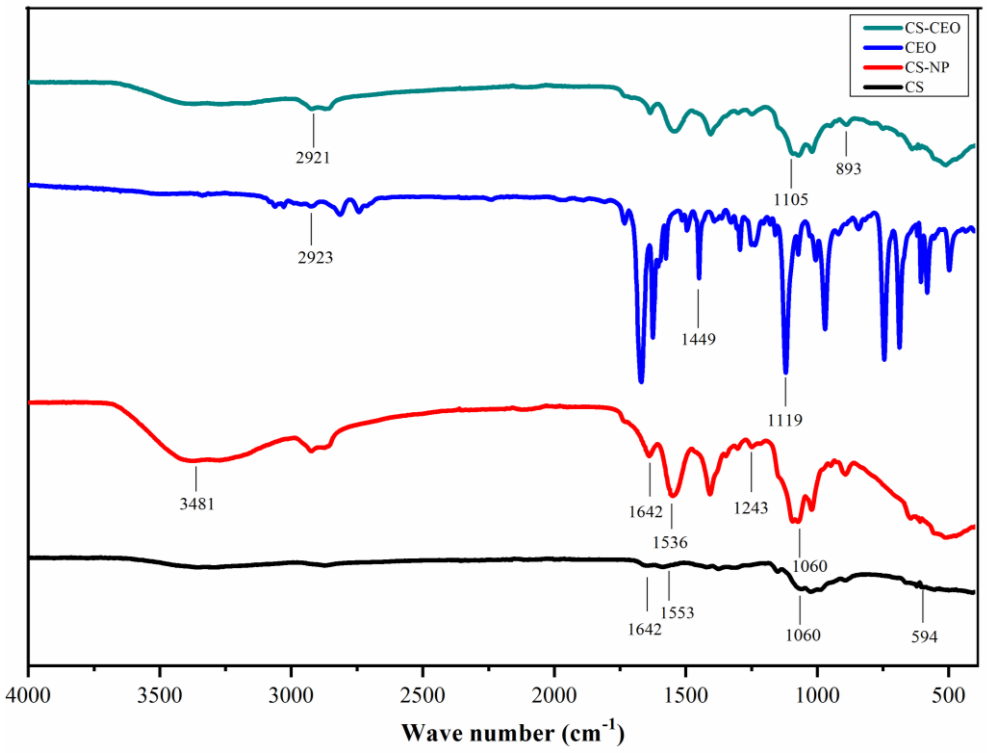

Figure 4. FT–IR spectra of CS, CS-NPs, CEO, and CS-CEO loaded at a CEO to CS weight ratio of 0.39:1.

The TGA thermograms of CS, pure CEO, CS-NP, and CS-CEO are presented in Figure 5a. CS exhibited two stages of weight loss: the first, from 60 to 120 °C, was ascribed to the adsorbed water; the second, from 185 to 330 °C, was due to the degradation of CS, dehydration of the glycoside rings, depolymerization, and decomposition of the acetylated and deacetylated units of CS. However, pure CEO only exhibited a single stage of weight loss: the temperature of its maximum degradation rate was 162 °C and it was almost completely degraded before 175 °C, which was compared with microcapsules. Thus, the thermal stability of EOs of microcapsules could be improved. CS-NPs exhibited distinct thermal characteristics from CS due to the crosslinking of CS and TPP [41].

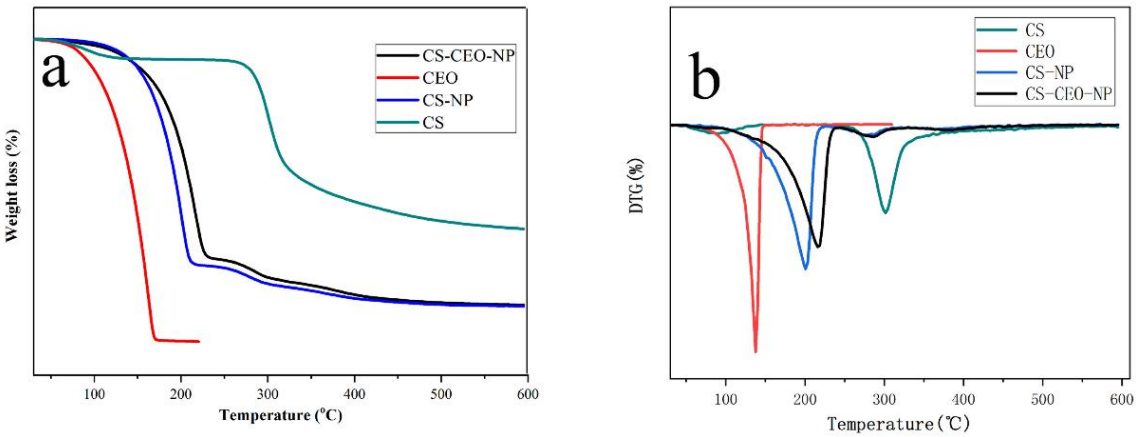

Figure 5. (**a**) TGA and (**b**) DTG thermograms of the CS powder, CEO, CS-NPs, and CS-CEO loaded at an initial CEO to CS weight ratio of 0.39:1.

Figure 5b presents the derivative thermogravimetry (DTG) curves. The DTG curve of CS-NPs displayed endothermic peaks at 200 and 279 °C and was increased to higher temperatures (218 and 281 °C) by the encapsulation of CEO. It was also observed that the embedded CEO (in CS-NPs) decomposed at a higher temperature (281 °C) than that of the free CEO (175 °C). These results may be

explained by the inclusion of CEOs in CS-NPs, and demonstrate that the thermal stability of CEOs was improved via encapsulation. This result indicates that CS-CEO can broaden the scope of CEO application in the food industry, which is in agreement with the results reported by Hadidi et al. [42].

The crystallographic structures of CS, CS-NPs, and CS-CEO are presented in Figure 6. CS exhibited two strong peaks at 2θ values of 10° and 20°, indicating a high degree of crystallinity. The two peaks of CS-NPs shifted to higher values of 11.69° and 22.8°, and the intensities of the peaks were significantly reduced, possibly because of the disruption of the crystal structure of CS after it was crosslinked with TPP. The width of the peaks was attributed to the crystallite size. Generally, the wider the peak, the lower is the degree of crystallinity [29]. The widest peak observed was for CS-CEO, compared to those of CS and CS-NPs, indicating that the encapsulation of CEO may have further reduced its crystallinity.

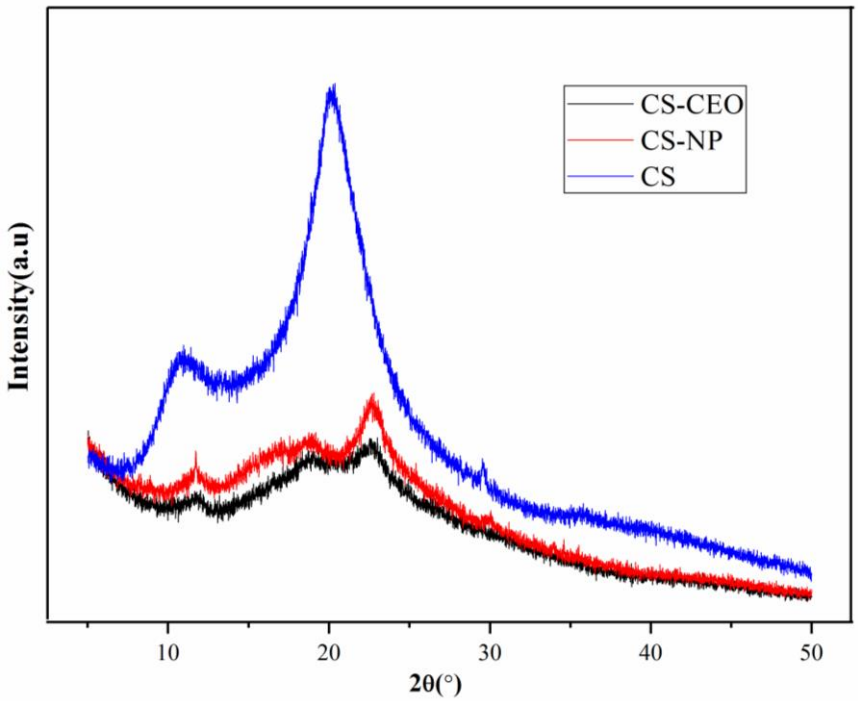

Figure 6. XRD patterns of the CS powder, CS-NPs, and CS-CEO loaded at an initial CEO to a CS weight ratio of 0.39:1.

3.3. AOA

It is well known that the DPPH free radical is very stable and can be stored for long periods. However, when it encounters a substance that can release a hydrogen atom (or being oxidized), the DPPH radical is eliminated. Consequently, the color of the compound in the solution changes from purple to light yellow. This reactivity is a suitable tool for the evaluation of the free radical scavenging activities of antioxidants [43,44]. Hydroxyl radicals are highly reactive free radicals in biological systems, and cause oxidative degradation of cell membrane lipids [45]. Herein, the AOA of bioactive CS-NPs containing the CEO was assessed by its percentage of DPPH and hydroxyl radical inhibition. The scavenging activities of CS-NPs containing different amounts of CEO are shown in Figure 7. As observed, the AOA of CS-CEO was higher than those of free CEO and CS. The percentage of scavenging activities of the DPPH and hydroxyl radicals displayed similar tendencies, increasing with an increase in the initial CEO content. The percentages of radical scavenging activities of the DPPH and hydroxyl radicals were in the ranges of 20.6–56.9% and 21.0–53.4%. However, at the highest addition of CEO (0.15 g) in both assays, their percentage of scavenging activities slightly decreased to 55.7% and 51.6%, respectively. At the highest EE (32.9%), the percentages of scavenging activities of both the DPPH

and hydroxyl radicals attained maxima of 56.9% and 53.4%. These results indicate that the radical scavenging activities reflected the variation in EE. A small amount of CS-CEO could significantly retain the AOA of CEO, and could be indirectly controlled as EE changes.

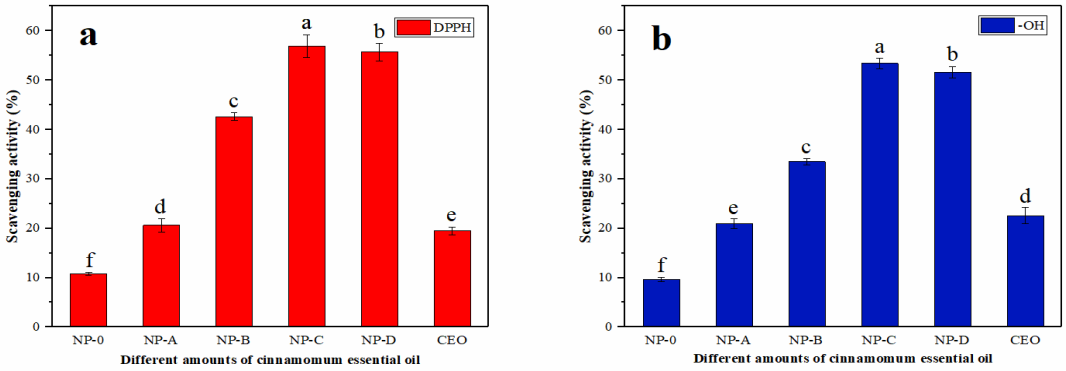

Figure 7. Scavenging activity of (**a**) DPPH and (**b**) -OH of CS-NPs loaded with different amounts of CEO (NP-0, NP-A, NP-B, NP-C, and NP-D with initial CEO to CS weight ratios of 0:1, 0.11:1, 0.25:1, 0.39:1, and 0.53:1, respectively). Bars with different letters are significantly different ($p < 0.05$).

The free radical scavenging activity of pure CEO has been reported in the literature. This effect is mainly due to the activities of some compounds, such as cinnamaldehyde and eugenol, which may be encapsulated in nanocapsules and employed as controlled release agents, displaying excellent AOA. In these studies [46,47], it was demonstrated that encapsulation improved the stability of many oxidation-sensitive substances and prevented the volatilization of their active ingredients. Thus, the AOA of bioactive compounds could be effectively protected by this encapsulation technique [48].

However, the DPPH and -OH free radical scavenging abilities of pure CEO were only 19.5% and 22.6%, which may be due to the instability of CEO in air, which affects its antioxidant capacity. Microcapsules can prevent EOs from being affected by external factors. In addition, CS has a certain antioxidant capacity, and the synergistic effect of CS and natural substances can have a good antioxidant effect [49].

4. Conclusions

CEO was successfully encapsulated in CS-NPs via oil-in-water emulsification and ionic gelation. The CS-CEO exhibited regular spherical shapes, the mean diameters of which ranged from 190 to 340 nm. The optimal EE of CS-CEO was obtained by utilizing a mixture of CS and CEO at a weight ratio of 1:0.39. The chemical structure, thermal stability, and crystallinity of the products were assessed by FT-IR, TGA, and XRD. A significant improvement was observed in terms of CEO stability. Through the DPPH and hydroxyl radical scavenging assays, it was found that their scavenging activities paralleled the EE of CS-CEO. CS-CEO significantly retained the AOA of the CEO, and could be indirectly controlled as the EE changed. These findings confirm that CEO can be effectively encapsulated in CS-NPs to further facilitate its utilization in the food industry.

Author Contributions: Conceptualization, C.H. and H.S.; methodology, H.S.; software, J.W.; validation, H.S., Y.L., and S.K.; formal analysis, H.H.; investigation, B.Z.; resources, Y.L.; data curation, H.S.; writing—original draft preparation, H.S.; writing—review and editing, H.S.; visualization, H.H.; supervision, J.W.; project administration, J.W.; funding acquisition, C.H. All authors have read and agreed to the published version of the manuscript.

Funding: This research was supported by the Guangxi Natural Science Foundation of China (grant number 2018AB45007).

Acknowledgments: The authors are grateful to the Institute of Light Industry and Food Engineering, Guangxi University, for supporting them with their large instrument platform.

Conflicts of Interest: The authors declare no conflict of interest.

References

1. Du, W.X.; Olsen, C.W.; Avena-Bustillos, R.J.; McHugh, T.H.; Levin, C.E.; Friedman, M. Effects of allspice, cinnamon, and clove bud essential oils in edible apple films on physical properties and antimicrobial activities. *J. Food Sci.* **2009**, *74*, M372–M378. [CrossRef] [PubMed]
2. Sarikurkcu, C.; Popovic-Djordjevic, J.; Solak, M.H. Wild edible mushrooms from Mediterranean region: Metal concentrations and health risk assessment. *Ecotoxicol. Environ. Saf.* **2020**, 190. [CrossRef] [PubMed]
3. Canan, I.; Gundogdu, M.; Seday, U.; Oluk, C.A.; Karasahin, Z.; Eroglu, E.C.; Yazici, E.; Unlu, M. Determination of antioxidant, total phenolic, total carotenoid, lycopene, ascorbic acid, and sugar contents of Citrus species and mandarin hybrids. *Turk. J. Agric.* **2016**, *40*, 894–899. [CrossRef]
4. Celik, A.; Ercisli, S.; Turgut, N. Some physical, pomological and nutritional properties of kiwifruit cv. Hayward. *Int. J. Food Sci. Nutr.* **2007**, *58*, 411–418. [CrossRef] [PubMed]
5. Sardeshpande, M.; Shackleton, C. Wild Edible Fruits: A Systematic Review of an Under-Researched Multifunctional NTFP (Non-Timber Forest Product). *Forests* **2019**, *10*, 467. [CrossRef]
6. Ercisli, S.; Tosun, M.; Duralija, B.; Voca, S.; Sengu, M.; Turan, M. Phytochemical Content of Some Black (*Morus nigra* L.) and Purple (*Morus rubra* L.) Mulberry Genotypes. *Food Technol. Biotech.* **2010**, *48*, 102–106.
7. Rop, O.; Ercisli, S.; Mlcek, J.; Jurikova, T.; Hoza, I. Antioxidant and radical scavenging activities in fruits of 6 sea buckthorn (*Hippophae rhamnoides* L.) cultivars. *Turk. J. Agric.* **2014**, *38*, 224–232. [CrossRef]
8. Zorenc, Z.; Veberic, R.; Stampar, F.; Koron, D.; Mikulic-Petkovsek, M. Changes in berry quality of northern highbush blueberry (*Vaccinium corymbosum* L.) during the harvest season. *Turk. J. Agric.* **2016**, *40*, 855–864. [CrossRef]
9. Mari, M.; Bautista-Banos, S.; Sivakumar, D. Decay control in the postharvest system: Role of microbial and plant volatile organic compounds. *Postharvest Biol. Technol.* **2016**, *122*, 70–81. [CrossRef]
10. Lee, J.; Park, G.; Chang, Y.H. Nutraceuticals and antioxidant properties of *Lonicera japonica* Thunb. as affected by heating time. *Int. J. Food Prop.* **2019**, *22*, 630–645. [CrossRef]
11. Wu, C.H.; Wang, L.P.; Hu, Y.Q.; Chen, S.G.; Liu, D.H.; Ye, X.Q. Edible coating from citrus essential oil-loaded nanoemulsions: Physicochemical characterization and preservation performance. *RSC Adv.* **2016**, *6*, 20892–20900. [CrossRef]
12. Kallel, I.; Hadrich, B.; Gargouri, B.; Chaabane, A.; Lassoued, S.; Gdoura, R.; Bayoudh, A.; Ben Messaoud, E. Optimization of Cinnamon (*Cinnamomum zeylanicum* Blume) Essential Oil Extraction: Evaluation of Antioxidant and Antiproliferative Effects. *Evid. Based Complement. Altern.* **2019**. [CrossRef] [PubMed]
13. Atares, L.; Bonilla, J.; Chiralt, A. Characterization of sodium caseinate-based edible films incorporated with cinnamon or ginger essential oils. *J. Food Eng.* **2010**, *100*, 678–687. [CrossRef]
14. Shan, B.; Cai, Y.Z.; Brooks, J.D.; Corke, H. Antibacterial properties and major bioactive components of cinnamon stick (*Cinnamomum burmannii*): Activity against foodborne pathogenic bacteria. *J. Agric. Food Chem.* **2007**, *55*, 5484–5490. [CrossRef]
15. Ayala-Zavala, J.F.; Silva-Espinoza, B.A.; Cruz-Valenzuela, M.R.; Leyva, J.M.; Ortega-Ramirez, L.A.; Carrazco-Lugo, D.K.; Perez-Carlon, J.J.; Melgarejo-Flores, B.G.; Gonzalez-Aguilar, G.A.; Miranda, M.R.A. Pectin-cinnamon leaf oil coatings add antioxidant and antibacterial properties to fresh-cut peach. *Flavour Frag. J.* **2013**, *28*, 39–45. [CrossRef]
16. Jamil, B.; Abbasi, R.; Abbasi, S.; Imran, M.; Khan, S.U.; Ihsan, A.; Javed, S.; Bokhari, H.; Imran, M. Encapsulation of Cardamom Essential Oil in Chitosan Nano-composites: In-vitro Efficacy on Antibiotic-Resistant Bacterial Pathogens and Cytotoxicity Studies. *Front. Microbiol.* **2016**, *7*. [CrossRef]
17. Ghaderi-Ghahfarokhi, M.; Barzegar, M.; Sahari, M.A.; Azizi, M.H. Nanoencapsulation Approach to Improve Antimicrobial and Antioxidant Activity of Thyme Essential Oil in Beef Burgers during Refrigerated Storage. *Food Bioprocess Technol.* **2016**, *9*, 1187–1201. [CrossRef]
18. Esmaeili, A.; Asgari, A. In vitro release and biological activities of Carum copticum essential oil (CEO) loaded chitosan nanoparticles. *Int. J. Biol. Macromol.* **2015**, *81*, 283–290. [CrossRef]
19. Dash, M.; Chiellini, F.; Ottenbrite, R.M.; Chiellini, E. Chitosan-A versatile semi-synthetic polymer in biomedical applications. *Prog. Polym. Sci.* **2011**, *36*, 981–1014. [CrossRef]
20. Huang, J.W.; Qin, J.Z.; Zhang, P.; Chen, X.M.; You, X.R.; Zhang, F.; Zuo, B.Q.; Yao, M. Facile preparation of a strong chitosan-silk biocomposite film. *Carbohydr. Polym.* **2020**, 229. [CrossRef]

21. Wei, S.; Ching, Y.C.; Chuah, C.H. Synthesis of chitosan aerogels as promising carriers for drug delivery: A review. *Carbohydr. Polym.* **2020**, *231*. [CrossRef] [PubMed]
22. Pillai, C.K.S.; Paul, W.; Sharma, C.P. Chitin and chitosan polymers: Chemistry, solubility and fiber formation. *Prog. Polym. Sci.* **2009**, *34*, 641–678. [CrossRef]
23. Yilmaz, M.T.; Yilmaz, A.; Akman, P.K.; Bozkurt, F.; Dertli, E.; Basahel, A.; Al-Sasi, B.; Taylan, O.; Sagdic, O. Electrospraying method for fabrication of essential oil loaded-chitosan nanoparticle delivery systems characterized by molecular, thermal, morphological and antifungal properties. *Innov. Food Sci. Emerg.* **2019**, *52*, 166–178. [CrossRef]
24. Khalili, S.T.; Mohsenifar, A.; Beyki, M.; Zhaveh, S.; Rahmani-Cherati, T.; Abdollahi, A.; Bayat, M.; Tabatabaei, M. Encapsulation of Thyme essential oils in chitosan-benzoic acid nanogel with enhanced antimicrobial activity against Aspergillus flavus. *LWT-Food Sci. Technol.* **2015**, *60*, 502–508. [CrossRef]
25. Mohammadi, A.; Hashemi, M.; Hosseini, S.M. Chitosan nanoparticles loaded with *Cinnamomum zeylanicum* essential oil enhance the shelf life of cucumber during cold storage. *Postharvest Biol. Tecnol.* **2015**, *110*, 203–213. [CrossRef]
26. Zhang, Y.B.; Liu, X.Y.; Wang, Y.F.; Jiang, P.P.; Quek, S. Antibacterial activity and mechanism of cinnamon essential oil against Escherichia coli and Staphylococcus aureus. *Food Control* **2016**, *59*, 282–289. [CrossRef]
27. Costa, E.M.; Silva, S.; Vicente, S.; Neto, C.; Castro, P.M.; Veiga, M.; Madureira, R.; Tavaria, F.; Pintado, M.M. Chitosan nanoparticles as alternative anti-staphylococci agents: Bactericidal, antibiofilm and antiadhesive effects. *Mater. Sci. Eng. C-Mater.* **2017**, *79*, 221–226. [CrossRef]
28. Feyzioglu, G.C.; Tornuk, F. Development of chitosan nanoparticles loaded with summer savory (*Satureja hortensis* L.) essential oil for antimicrobial and antioxidant delivery applications. *LWT-Food Sci. Technol.* **2016**, *70*, 104–110. [CrossRef]
29. Hosseini, S.F.; Zandi, M.; Rezaei, M.; Farahmandghavi, F. Two-step method for encapsulation of oregano essential oil in chitosan nanoparticles: Preparation, characterization and in vitro release study. *Carbohydr. Polym.* **2013**, *95*, 50–56. [CrossRef]
30. Bala, A.; Singh, B. Concomitant production of cellulase and xylanase by thermophilic mould Sporotrichum thermophile in solid state fermentation and their applicability in bread making. *World J. Microbiol. Biotechnol.* **2017**, 33. [CrossRef]
31. Pan, J.F.; Shen, H.X.; Luo, Y.K. Cryoprotective Effects of Trehalose on Grass Carp (*Ctenopharyngodon Idellus*) Surimi during Frozen Storage. *J. Food Process. Preserv.* **2010**, *34*, 715–727. [CrossRef]
32. Carvalho, R.L.; Cabral, M.F.; Germano, T.A.; de Carvalho, W.M.; Brasil, I.M.; Gallao, M.I.; Moura, C.F.H.; Lopes, M.M.A.; de Miranda, M.R.A. Chitosan coating with trans-cinnamaldehyde improves structural integrity and antioxidant metabolism of fresh-cut melon. *Postharvest Biol. Technol.* **2016**, *113*, 29–39. [CrossRef]
33. Dong, H.M.; Zhang, Q.; Li, L.; Liu, J.; Shen, L.W.; Li, H.Y.; Qin, W. Antioxidant activity and chemical compositions of essential oil and ethanol extract of Chuanminshen violaceum. *Ind. Crop. Prod.* **2015**, *76*, 290–297. [CrossRef]
34. Vilas, V.; Philip, D.; Mathew, J. Essential oil mediated synthesis of silver nanocrystals for environmental, anti-microbial and antioxidant applications. *Mater. Sci. Eng. C-Mater.* **2016**, *61*, 429–436. [CrossRef]
35. Kavaz, D.; Idris, M.; Onyebuchi, C. Physiochemical characterization, antioxidative, anticancer cells proliferation and food pathogens antibacterial activity of chitosan nanoparticles loaded with Cyperus articulatus rhizome essential oils. *Int. J. Biol. Macromol.* **2019**, *123*, 837–845. [CrossRef]
36. Abreu, F.O.M.S.; Oliveira, E.F.; Paula, H.C.B.; de Paula, R.C.M. Chitosan/cashew gum nanogels for essential oil encapsulation. *Carbohydr. Polym.* **2012**, *89*, 1277–1282. [CrossRef] [PubMed]
37. Donsi, F.; Annunziata, M.; Sessa, M.; Ferrari, G. Nanoencapsulation of essential oils to enhance their antimicrobial activity in foods. *LWT-Food Sci. Technol.* **2011**, *44*, 1908–1914. [CrossRef]
38. Bai, Z.F.; Cristancho, D.E.; Rachford, A.A.; Reder, A.L.; Williamson, A.; Grzesiak, A.L. Controlled Release of Antimicrobial ClO2 Gas from a Two-Layer Polymeric Film System. *J. Agric. Food Chem.* **2016**, *64*, 8647–8652. [CrossRef] [PubMed]
39. Ray, S.; Jin, T.; Fan, X.T.; Liu, L.S.; Yam, K.L. Development of Chlorine Dioxide Releasing Film and Its Application in Decontaminating Fresh Produce. *J. Food Sci.* **2013**, *78*, M276–M284. [CrossRef]

40. Luque-Alcaraz, A.G.; Cortez-Rocha, M.O.; Velazquez-Contreras, C.A.; Acosta-Silva, A.L.; Santacruz-Ortega, H.D.; Burgos-Hernandez, A.; Arguelles-Monal, W.M.; Plascencia-Jatomea, M. Enhanced Antifungal Effect of Chitosan/Pepper Tree (Schinus molle) Essential Oil Bionanocomposites on the Viability of Aspergillus parasiticus Spores. *J. Nanomater.* **2016**. [CrossRef]
41. Woranuch, S.; Yoksan, R. Eugenol-loaded chitosan nanoparticles: I. Thermal stability improvement of eugenol through encapsulation. *Carbohydr. Polym.* **2013**, *96*, 578–585. [CrossRef] [PubMed]
42. Hadidi, M.; Pouramin, S.; Adinepour, F.; Haghani, S.; Jafari, S.M. Chitosan nanoparticles loaded with clove essential oil: Characterization, antioxidant and antibacterial activities. *Carbohydr. Polym.* **2020**, 236. [CrossRef] [PubMed]
43. Chen, H.P.; Zhao, M.M.; Lin, L.Z.; Wang, J.F.; Sun-Waterhouse, D.X.; Dong, Y.; Zhuang, M.Z.; Su, G.W. Identification of antioxidative peptides from defatted walnut meal hydrolysate with potential for improving learning and memory. *Food Res. Int.* **2015**, *78*, 216–223. [CrossRef] [PubMed]
44. Carrasco, A.; Tomas, V.; Tudela, J.; Miguel, M.G. Comparative study of GC-MS characterization, antioxidant activity and hyaluronidase inhibition of different species of Lavandula and Thymus essential oils. *Flavour Frag. J.* **2016**, *31*, 57–69. [CrossRef]
45. Takshak, S.; Agrawal, S.B. The role of supplemental ultraviolet-B radiation in altering the metabolite profile, essential oil content and composition, and free radical scavenging activities of *Coleus forskohlii*, an indigenous medicinal plant. *Environ. Sci. Pollut. Res.* **2016**, *23*, 7324–7337. [CrossRef]
46. Qiu, C.; Chang, R.R.; Yang, J.; Ge, S.J.; Xiong, L.; Zhao, M.; Li, M.; Sun, Q.J. Preparation and characterization of essential oil-loaded starch nanoparticles formed by short glucan chains. *Food Chem.* **2017**, *221*, 1426–1433. [CrossRef]
47. Wang, Y.F.; Xia, Y.W.; Zhang, P.Y.; Ye, L.; Wu, L.Q.; He, S.K. Physical Characterization and Pork Packaging Application of Chitosan Films Incorporated with Combined Essential Oils of Cinnamon and Ginger. *Food Bioprocess Technol.* **2017**, *10*, 503–511. [CrossRef]
48. Zhaveh, S.; Mohsenifar, A.; Beiki, M.; Khalili, S.T.; Abdollahi, A.; Rahmani-Cherati, T.; Tabatabaei, M. Encapsulation of Cuminum cyminum essential oils in chitosan-caffeic acid nanogel with enhanced antimicrobial activity against Aspergillus flavus. *Ind. Crop. Prod.* **2015**, *69*, 251–256. [CrossRef]
49. Wong, L.W.; Loke, X.J.; Chang, C.K.; Ko, W.C.; Hou, C.Y.; Hsieh, C.W. Use of the plasma-treated and chitosan/gallic acid-coated polyethylene film 2 for the preservation of tilapia (*Orechromis niloticus*) fillets. *Food Chem.* **2020**, 329. [CrossRef]